

06;10

Linked orientation effects and a large anisotropy of effective parameters of novel 2–1–2 composites based on ferroelectrics

© V.Yu. Topolov

Southern Federal University, Rostov-on-Don, Russia
E-mail: vutopolov@sfedu.ru

Received February 26, 2024

Revised April 15, 2024

Accepted April 15, 2024

Orientation dependences of electromechanical coupling factors k_{3j}^* , squared figures of merit $(Q_{3j}^*)^2$ and their anisotropy factors are studied in the 2–1–2 composites at rotations of the main crystallographic axes of [011]-poled ferroelectric single crystal and bases of ferroelectric ceramic rods. Validity of the large-anisotropy conditions $|k_{33}^*/k_{3f}^*| \geq 5$ and $(Q_{33}^*/Q_{3f}^*)^2 \geq 10$ is analyzed by considering two rotation modes in the composites based on one of single crystals, $0.935\text{Pb}(\text{Zn}_{1/3}\text{Nb}_{2/3})\text{O}_3-0.065\text{PbTiO}_3$ or $0.72\text{Pb}(\text{Mg}_{1/3}\text{Nb}_{2/3})\text{O}_3-0.28\text{PbTiO}_3$. Results are to be taken into account when creating high-effective piezo-active composites for transducers, sensors, acoustic and energy-harvesting devices.

Keywords: piezo-active composite, orientation dependences, anisotropy, electromechanical coupling factor, figure of merit.

DOI: 10.61011/TPL.2024.08.58909.19906

Composites based on ferroelectrics (FEs) [1–3] with 2–2 and 1–3 connectivities are in high demand at present, and modifications of the structures of such composites [4,5] contribute to the enhancement of certain parameters for practical applications relying on the piezoelectric effect. These parameters include the electromechanical coupling factors (ECFs) [1–3.5] and squared figures of merit (SFMs) [4], which are associated with energy conversion due to the piezoelectric effect. The three-component composite with 2–1–2 connectivity, which has been proposed recently in [4], is characterized by a combination of 2–2 and 1–3 connectivity elements that have been often considered separately in various composite structures examined earlier. The combined influence of 2–2 and 1–3 structures and orientation effects on the effective physical properties and related parameters of various 2–1–2 composites remains understudied. The aim of the present study is to analyze the orientation effects and factors inducing a large anisotropy of ECFs and SFMs in 2–1–2 FE crystal–FE ceramic–polymer composites.

It is assumed that parallel-connected layers of a 2–1–2 composite (Fig. 1) are distributed periodically along the OX_1 axis. The first (main) FE component is a polydomain crystal (inset *a* in Fig. 1). Its main crystallographic axes X , Y , and Z satisfy conditions $X \parallel [0\bar{1}1] \parallel OX_1$, $Y \parallel [100] \parallel OX_2$, $Z \parallel [011] \parallel \mathbf{P}_s^{(1)} \parallel OX_3$. The second FE component is a system of long ceramic rods parallel to the OX_3 axis with residual polarization $\mathbf{P}_r^{(2)} \parallel OX_3$. These rods are shaped like elliptical cylinders and arranged periodically in the polymer matrix (inset *b* in Fig. 1), forming a 1–3 structure within the layers adjacent to the crystalline layers. The OX_3 axis is the polarization axis of the 2–1–2 composite. The rotation of main crystallographic axes X , Y around $Z \parallel OX_3$ by angle

α (inset *a* in Fig. 1) and the rotation of elliptical bases of ceramic rods around OX_3 by angle γ (inset *b* in Fig. 1) are performed counterclockwise (viewed from the tip of axis OX_3) in all the layers.

The effective electromechanical properties (i.e., a complete set of dielectric, piezoelectric, and elastic properties) of the 2–1–2 composite were determined in four stages. The first stage involves the determination of the crystal properties as functions of rotation angle α . At the second stage, the properties of the ceramic–polymer layer (1–3 structure) are characterized using the effective field method [6] at $\gamma = 0^\circ$ (inset *b* in Fig. 1) as functions of the volume fraction m_c of ceramic rods and ratio $\eta_c = a_1/a_2$ of the lengths of semiaxes of the rod base. At the third stage, the properties of the ceramic–polymer layer are determined with account for the rotation of the rod bases by angle γ . The fourth stage involves the determination of the effective properties of the 2–1–2 composite with the use of the matrix method [4,7] that is applicable to a 2–2 structure within the $0 < m < 1$ range of crystal volume fractions.

ECFs

$$k_{3j}^* = d_{3j}^*/(\varepsilon_{33}^{*\sigma} s_{jj}^{*E})^{1/2} \quad (1)$$

and SFMs

$$(Q_{3j}^*)^2 = d_{3j}^* g_{3j}^* \quad (2)$$

examined here depend on m , m_c , η_c , α , and γ . In formula (1), d_{3j}^* is the piezoelectric coefficient, $\varepsilon_{33}^{*\sigma}$ is the permittivity at mechanical stress $\sigma = \text{const}$, and s_{jj}^{*E} is the elastic compliance in electric field $E = \text{const}$. Piezocoefficients g_{3j}^* from (2) may be determined [7] as $d_{fk}^* = \varepsilon_{fj}^{*\sigma} g_{jk}^*$. SFMs $(Q_{3j}^*)^2$ from (2) characterize the signal-to-noise ratio in applications involving the longitudinal ($j = 3$) or transverse ($j = 1, 2$) piezoelectric effect [7].

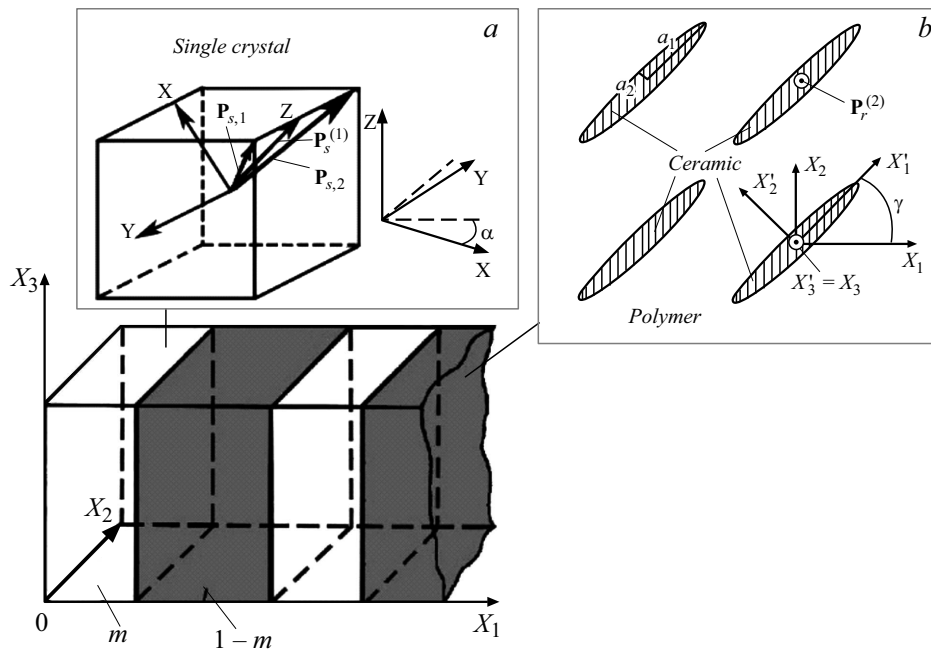


Figure 1. Schematic diagram of a 2–1–2 composite with two FE components. $(X_1X_2X_3)$ — rectangular coordinate system; m and $1-m$ — volume fractions of the FE crystal and FE ceramic–polymer layers, respectively; $\mathbf{P}_s^{(1)}$ — spontaneous polarization of the FE crystal; and $\mathbf{P}_{s,i}$ — spontaneous polarization of a domain of type i in the FE crystal.

Effective parameters (1), (2) were examined for 2–1–2 composites based on [011]-poled crystals of one of the following relaxor ferroelectrics: $0.935\text{Pb}(\text{Zn}_{1/3}\text{Nb}_{2/3})\text{O}_3-0.065\text{PbTiO}_3$ (PZN–0.065PT, the values of elastic compliances s_{ab}^E , piezoelectric coefficients d_{ij} , and permittivities ε_{pp}^σ were taken from [8]) and $0.72\text{Pb}(\text{Mg}_{1/3}\text{Nb}_{2/3})\text{O}_3-0.28\text{PbTiO}_3$ (PMN–0.28PT, the values of s_{ab}^E , d_{ij} , and ε_{pp}^σ were taken from [9]). Both composites contain FE ceramic $\text{Li}_{0.03}(\text{K}_{0.48}\text{Na}_{0.52})_{0.97}(\text{Nb}_{0.8}\text{Ta}_{0.2})\text{O}_3$ (KNNLT, the values of elastic moduli c_{ab}^E , piezocoefficients e_{ij} , and permittivities $\varepsilon_{pp}^\varepsilon$ were taken from [10]) and polyethylene (PE) [7]. Taking into account the macroscopic symmetry of components and the composite as a whole, one may rewrite formula (2) as $(Q_{3j}^*)^2 = (d_{3j}^*)^2/\varepsilon_{33}^{*\sigma}$.

Examples of orientation dependences of the effective piezoelectric properties, ECFs, and SFMs are presented in Fig. 2. These data are valid for composites with a large length ratio ($\eta_c = 100$) of semiaxes of the elliptical cross section of the rods. At volume fractions $m_c \ll 1$ of the FE ceramic material, the ceramic–polymer layer then exhibits a significant anisotropy of elastic and piezoelectric properties.

Analyzing Figs. 2, *a* and *b*, one may note that, compared to the rotation of the bases of the ceramic rods, the rotation of main crystallographic axes X, Y of the crystal leads to more noticeable changes in the ECFs k_{31}^* and k_{32}^* of the composite. This difference is attributable to the piezoelectric activity of the FE crystal, which is higher than the piezoelectric activity of the FE ceramic–polymer layer, and to a sign change of piezoelectric coefficient d'_{32}

of the PZN–0.065PT crystal near $\alpha = 56^\circ$. It is also worth noting that piezoelectric coefficients $d'_{31} = -1430$ pC/N and $d'_{33} = 1570$ pC/N of the PZN–0.065PT crystal at $\alpha = 56^\circ$ differ by just 9.8% in magnitude. These factors contribute to sign changes of ECFs k_{31}^* , k_{32}^* (Figs. 2, *a, b*) and piezoelectric coefficients d_{31}^* , d_{32}^* of the composites (curves 1, 2 in Fig. 2, *c*) at certain angles α^* , which vary with volume fractions m and m_c . The monotonic increase of ECFs k_{31}^* and $|k_{32}^*|$ within the $0 \leq \gamma \leq 90^\circ$ interval (Fig. 2, *b*) is closely associated with monotonic variations of piezoelectric coefficients d_{3j}^* and elastic compliances s_{11}^{*E} , s_{22}^{*E} . The constancy of ECFs k_{33}^* under variation of angle γ at $m = \text{const}$ and $m_c = \text{const}$ (curves 3 and 6 in Fig. 2, *b*) stems from the lack of factors causing changes in the longitudinal response of the composite (d_{33}^* , $\varepsilon_{33}^{*\sigma}$, and s_{33}^{*E} in formula (1)) for this rotation mode.

The plots in Figs. 2, *c–e* correspond to composites with ceramic–polymer layers exerting (owing to a high volume fraction; $1-m \gg m$), a significant influence on angles α^* . Variations of effective parameters d_{3f}^* , g_{3f}^* , and $(Q_{3f}^*)^2$ ($f = 1, 2$) are induced either by a substitution of the crystalline component (cf. Figs. 2, *c* and *d*) or an increase in volume fraction m_c of the KNNLT ceramic material in the above-mentioned layers (cf. Figs. 2, *d* and *e*). By comparison, the $d'_{32} = 0$ condition in the PMN–0.28PT crystal is fulfilled near $\alpha = 58^\circ$, and piezoelectric coefficients $d'_{31} = -702$ pC/N and $d'_{33} = 860$ pC/N differ in magnitude by approximately 23%. The smaller values of d'_{33} and $|d'_{31}|$ in PMN–0.28PT are the reason why the effective parameters of this composite are lower than

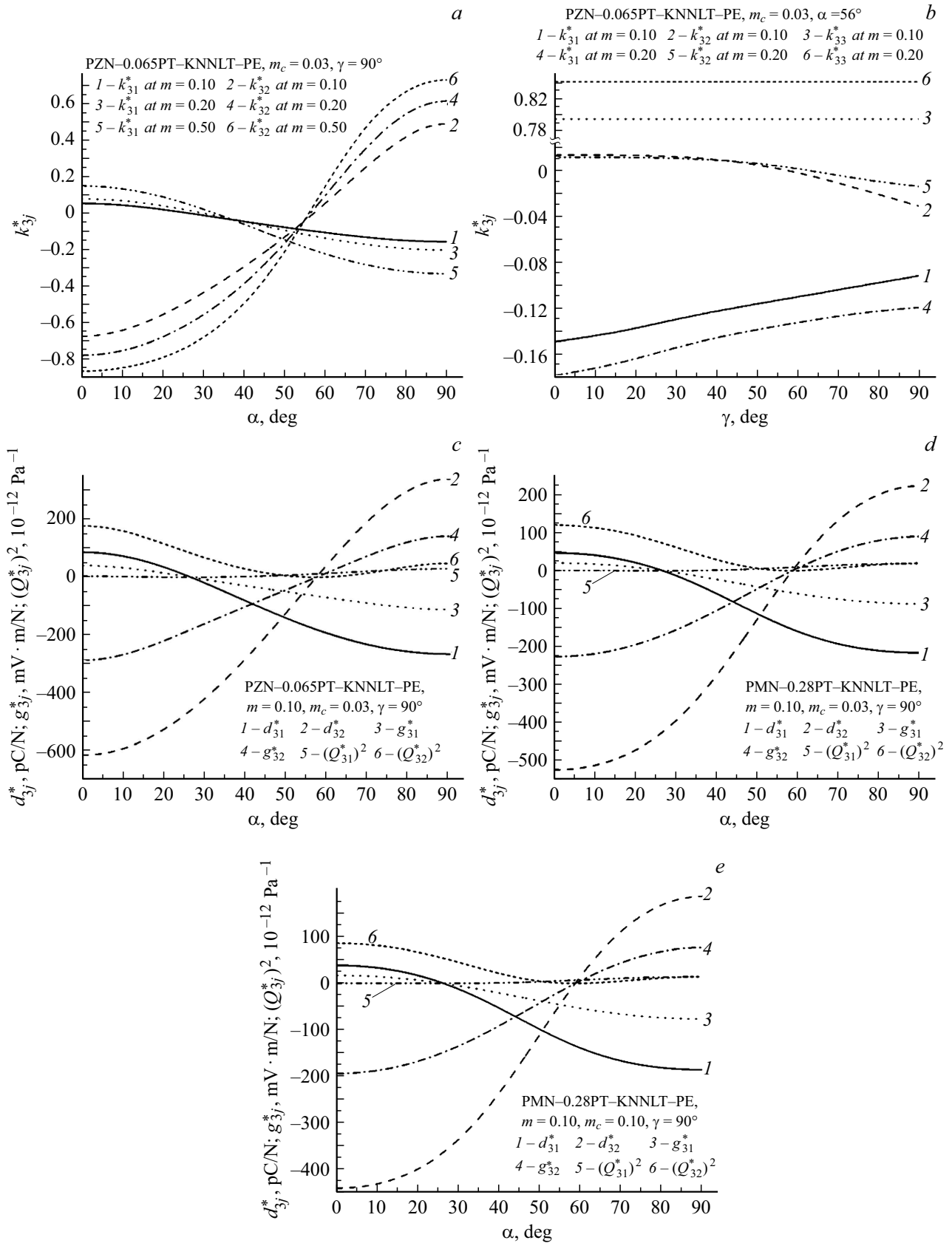


Figure 2. Orientation dependences of ECFs k_{3j}^* (a,b), piezoelectric coefficients d_{3j}^* , piezocoefficients g_{3j}^* , and SFMs $(Q_{3j}^*)^2$ (c-e) of 2-1-2 composites as follows: PZN crystal-0.065PT-KNNLT ceramic-polyethylene (a-c) and PMN crystal-0.28PT-KNNLT ceramic-polyethylene (d, e). The volume fraction of the KNNLT ceramic is $m_c = 0.03$ (a-d) or 0.10 (e).

The highest volume fractions m_{k-up} and m_{Q-up} of the crystal satisfying conditions (3) and (4), respectively, in 2–1–2 composites at $m_c = 0.03$

$\alpha, ^\circ$	$\gamma = 0^\circ$		$\gamma = 30^\circ$		$\gamma = 60^\circ$		$\gamma = 90^\circ$	
	m_{k-up}	m_{Q-up}	m_{k-up}	m_{Q-up}	m_{k-up}	m_{Q-up}	m_{k-up}	m_{Q-up}
PZN–0.065PT–KNNLT ceramic–polyethylene composite								
51	0.290	0.154	0.466	0.166	0.479	0.195	0.424	0.221
52	0.253	0.133	0.423	0.134	0.538	0.157	0.563	0.193
53	0.220	0.115	0.383	0.106	0.501	0.125	0.529	0.169
PMN–0.28PT–ceramic KNNLT–polyethylene composite								
55	0.515	0.121	0.653	0.112	0.735	0.125	0.752	0.165
56	0.485	0.107	0.628	0.090	0.715	0.099	0.733	0.144
57	0.456	0.094	0.602	0.070	0.694	0.075	0.714	0.124

those of PZN–0.065PT (cf. Figs. 2, *c* and *d*). As the volume fraction m_c increases, elastic compliances $|s_{ab,c-p}^E|$ of the ceramic–polymer layer decrease, thus restricting the growth of transverse piezoelectric coefficients $|d_{3f}^*|$, piezocoefficients $|g_{3f}^*|$, and SFM $(Q_{3f}^*)^2$ (cf. Figs. 2, *d* and *e* at $\alpha = \text{const}$). The rotation of the bases of the ceramic rods by angle $\gamma = 90^\circ$ contributes to weakening of the piezoelectric effect along axes OX_1 and OX_2 via individual elastic compliances $s_{ab,c-p}^E$.

The conditions for a large anisotropy of ECFs

$$|k_{33}^*/k_{31}^*| \geq 5, \quad |k_{33}^*/k_{32}^*| \geq 5 \quad (3)$$

and SFMs

$$(Q_{33}^*/Q_{31}^*)^2 \geq 10, \quad (Q_{33}^*/Q_{32}^*)^2 \geq 10 \quad (4)$$

are satisfied within the crystal volume fraction ranges of $[m_{k-low}; m_{k-up}]$ and $[m_{Q-low}; m_{Q-up}]$ respectively. Analyzing expressions (3) with (1) taken into account, one finds that elastic compliances s_{11}^E , s_{22}^E , and s_{33}^E are instrumental in forming the large k_{3j}^* anisotropy. The anisotropy of piezoelectric coefficients d_{3j}^* affects the fulfillment of all conditions (3), (4). Coupled orientation effects in 2–1–2 composites enable efficient energy conversion along the OX_3 polarization axis. The ceramic–polymer layers have a significant effect on the fulfillment of conditions (3) and (4), and the lower boundary of crystal volume fractions for both composites is $m_{k-low} = m_{Q-low} = 0.001$. Upper volume fraction boundaries m_{k-up} and m_{Q-up} vary with the crystal type and angles α and γ (see the table), providing high values of longitudinal ECF k_{33}^* and SFM $(Q_{33}^*)^2$. For example, the composite based on PZN–0.065PT at $\alpha = 52^\circ$ and $m = 0.20$ has $k_{33}^* = 0.841$ and $(Q_{33}^*)^2 = 110 \cdot 10^{-12} \text{ Pa}^{-1}$; i.e., $0.934k_{33}$ and $2.15(Q_{33})^2$ (the quantities without asterisks correspond to the crystal). The values of $k_{33}^* = 0.841 = 0.947k_{33}$ and $(Q_{33}^*)^2 = 80.2 \cdot 10^{-12} \text{ Pa}^{-1} = 3.72(Q_{33})^2$ were determined for the composite based on PMN–0.28PT at $\alpha = 56^\circ$ and $m = 0.14$. The indicated values of SFM $(Q_{33}^*)^2$ of both composites are higher than SFM $(Q_{33})^2 = 59 \cdot 10^{-12} \text{ Pa}^{-1}$ [11] of textured $\text{Pb}(\text{Mg}_{1/3}\text{Nb}_{2/3})\text{O}_3\text{–PbZrO}_3\text{–PbTiO}_3$ ceramic.

The study on the 2–1–2 composites with two FE components illustrates the important role of coupled orientation effects in the formation of piezoelectric properties (ECFs k_{3j}^* from (1) and SFMs $(Q_{3j}^*)^2$ from (2)). Rotation angles $50 < \alpha < 60^\circ$ and $\gamma = 90^\circ$ contribute to the large ECF and SFM anisotropy via the variation of the anisotropy of the elastic and piezoelectric properties of composite layers and a change in sign of the piezoelectric coefficient d'_{32} of the [011]-poled crystal. The fulfillment of conditions (3) and (4) in sufficiently wide ranges of crystal volume fractions m at ceramic fractions $m_c \ll 1$ should be taken into account in the development of new composites with 1–3 and 2–2 connectivity elements for piezoelectric transducers, sensors, and elements of acoustic, energy-saving, and other devices.

Funding

This study was supported by the Southern Federal University (contract 176/22-D dated July 11, 2022).

Conflict of interest

The author declares that he has no conflict of interest.

References

- [1] Z. Ma, N. Jia, C. Li, L. Ning, Y. Dang, H. Du, F. Li, Z. Xu, *Mater. Lett.*, **353**, 135284 (2023). DOI: 10.1016/j.matlet.2023.135284
- [2] H. Qin, H. Lu, X. Shen, Z. Xin, B. Yang, *Sensors Actuators A*, **366**, 115024 (2024). DOI: 10.1016/j.sna.2024.115024
- [3] L. Ning, N. Jia, C. Wang, Z. Ma, Y. Dang, C. Sun, H. Du, Z. Xu, F. Li, *Sensors Actuators A*, **367**, 115023 (2024). DOI: 10.1016/j.sna.2024.115023
- [4] V.Yu. Topolov, *Smart Mater. Struct.*, **32** (8), 085010 (2023). DOI: 10.1088/1361-665X/acdc4
- [5] J. Zhang, J. Wang, C. Zhong, L. Qin, *Compos. Struct.*, **32**, 117406 (2023). DOI: 10.1016/j.compstruct.2023.117406
- [6] J.H. Huang, W.-S. Kuo, *J. Appl. Phys.*, **81** (3), 1378 (1997). DOI: 10.1063/1.363874

- [7] J.I. Roscow, V.Yu. Topolov, C.R. Bowen, H. Khanbarez, *Innovative piezo-active composites and their structure–property relationships* (World Scientific, Singapore, 2022), p. 9, 76–81. DOI: 10.1142/13003
- [8] S. Zhang, L.C. Lim, *AIP Adv.* **8** (11), 115010 (2018). DOI: 10.1063/1.5064418
- [9] G. Liu, W. Jiang, J. Zhu, W. Cao, *Appl. Phys. Lett.*, **99** (16), 162901 (2011). DOI: 10.1063/1.3652703
- [10] F.-Z. Yao, K. Wang, J.-F. Li, *J. Appl. Phys.*, **113** (17), 174105 (2013). DOI: 10.1063/1.4803711
- [11] Y. Yan, K.-H. Cho, D. Maurya, A. Kumar, S. Kalinin, A. Khachatryan, S. Priya, *Appl. Phys. Lett.*, **102** (4), 042903 (2013). DOI: 10.1063/1.4789854

Translated by D.Safin